Gex1 is a yeast glutathione exchanger that interferes with pH and redox homeostasis

Manel Dhaoui[a,b], Françoise Auchère[c], Pierre-Louis Blaiseau[c], Emmanuel Lesuisse[c], Ahmed Landoulsi[b], Jean-Michel Camadro[c], Rosine Haguenauer-Tsapis[a], and Naïma Belgareh-Touzé[a,*]

[a]Laboratoire Ubiquitine et Trafic Intracellulaire, Institut Jacques Monod, UMR 7592 CNRS-Université Paris-Diderot, Paris, France; [b]Laboratoire de Biochimie et Biologie Moléculaire 03/UR/0902, Faculté des Sciences de Bizerte, Zarzouna, Tunisia; [c]Laboratoire Mitochondries, Métaux et Stress Oxydatif, Institut Jacques Monod, UMR 7592 CNRS-Université Paris-Diderot, Paris, France

ABSTRACT **In the yeast *Saccharomyces cerevisiae*, glutathione plays a major role in heavy metal detoxification and protection of cells against oxidative stress. We show that Gex1 is a new glutathione exchanger. Gex1 and its paralogue Gex2 belong to the major facilitator superfamily of transporters and display similarities to the Aft1-regulon family of siderophore transporters. Gex1 was found mostly at the vacuolar membrane and, to a lesser extent, at the plasma membrane. Gex1 expression was induced under conditions of iron depletion and was principally dependent on the iron-responsive transcription factor Aft2. However, a *gex1*Δ *gex2*Δ strain displayed no defect in known siderophore uptake. The deletion mutant accumulated intracellular glutathione, and cells overproducing Gex1 had low intracellular glutathione contents, with glutathione excreted into the extracellular medium. Furthermore, the strain overproducing Gex1 induced acidification of the cytosol, confirming the involvement of Gex1 in proton transport as a probable glutathione/proton antiporter. Finally, the imbalance of pH and glutathione homeostasis in the *gex1*Δ *gex2*Δ and Gex1-overproducing strains led to modulations of the cAMP/protein kinase A and protein kinase C1 mitogen-activated protein kinase signaling pathways.**

Monitoring Editor
Jeffrey L. Brodsky
University of Pittsburgh

Received: Nov 19, 2010
Revised: Mar 18, 2011
Accepted: Apr 7, 2011

INTRODUCTION

The metabolism of oxygen in cells leads to the generation of reactive oxygen species (ROS), such as hydrogen peroxide (H_2O_2), the superoxide anion ($O_2^{\cdot -}$), and the hydroxyl free radical ($OH^{\cdot}$). ROS are inevitable by-products of oxygen metabolism but, at high concentration, they can cause oxidative damage to the cell, including protein oxidation, lipid peroxidation, and chromatin breaks (for reviews see Scandalios, 2002; Pocsi *et al.*, 2004; Wysocki and Tamás, 2010).

Thiol-containing molecules play an essential role in protecting cells against oxidative damage. They react with ROS, resulting in the neutralization of these potentially dangerous molecules. In most living organisms, the tripeptide glutathione (γ-L-glutamyl-L-cysteinyl-glycine: GSH in its reduced form, GSSG in its oxidized form) is the most abundant low–molecular weight, thiol-containing molecule. Glutathione is a strong cellular redox buffer due to its low redox potential ($E_0^{'}$ = –240 mV), its high redox ratio (GSH:GSSG) of 16:1, and its high cellular concentration (1–10 mM) (Grant *et al.*, 1996; Penninckx, 2002). Yeast cells grown in normal aerobic conditions have a high redox ratio (90% of glutathione in the reduced form), which is maintained through strict regulation of glutathione biosynthesis—mediated by glutathione synthetase (Gsh1 and Gsh2)—and of glutathione reduction, mediated by glutathione reductase (Glr1) in an NADPH-dependent reaction (Herrero *et al.*, 2008). GSH is also involved in the detoxification of xenobiotics and resistance to heavy metal stress. This detoxification capacity is due to the highly nucleophilic properties of the thiol moiety of GSH. The role of glutathione in cadmium detoxification is well documented. Cadmium has been shown to react with two molecules of GSH to form a stable GS-Cd-SG conjugate (Polec-Pawlak *et al.*, 2007). In *Saccharomyces cerevisiae*, this complex is removed from the cytosol by ATP-dependent

This article was published online ahead of print in MBoC in Press (http://www.molbiolcell.org/cgi/doi/10.1091/mbc.E10-11-0906) on April 13, 2011.

*Present address: Institut de Biologie Physico-Chimique, FRE 3354 CNRS/UPMC, Université Paris 06, Paris, France.

Address correspondence to: Naïma Belgareh-Touzé (belgareh@ibpc.fr).

Abbreviations used: ARN, Aft1 regulon; BPS, bathophenanthroline bisulfonic acid; EN, enterobactin; FCH, ferrichrome; FOB, ferrioxamine B; GSH, reduced glutathione; GSSG, oxidized glutathione; MFS, major facilitator superfamily; MRP, multidrug resistance–associated protein; MVBs, multivesicular bodies; OATP, organic anion-transporting polypeptide; ROS, reactive oxygen species; TAF, triacetylfusarinine; TGN, *trans*-Golgi network.

glutathione S–conjugate export pumps (GS-X pumps), such as Ycf1, a vacuolar membrane protein that imports $Cd(GS)_2$ into the vacuolar lumen, and Yor1, a plasma membrane protein that exports $Cd(GS)_2$ from cells (Szczypka *et al.*, 1994; Li *et al.*, 1996; Ghosh *et al.*, 1999; Gueldry *et al.*, 2003; Nagy *et al.*, 2006; Paumi *et al.*, 2009).

In mammalian cells, GSH conjugates are transported by ATP-binding cassette proteins of the multidrug resistance–associated protein (MRP) family and by proteins of the organic anion–transporting polypeptide (OATP) family (Homolya *et al.*, 2003; Ballatori *et al.*, 2005). Six of the 12 members of the MRP family (MRP1–5 and cystic fibrosis transmembrane conductance regulator) have been shown to mediate glutathione-conjugate extrusion at the plasma membrane. OATP transporters function without ATP and are less well characterized. OATP transporters were originally characterized as uptake transporters, but some are probably involved in glutathione efflux from the cell.

Given the importance of glutathione in redox ratio maintenance and detoxification, the genes involved in the biosynthesis, metabolism, and transport of glutathione are tightly controlled. Exposure to oxidative stress or to heavy metals leads to activation of the stress response regulators Yap1 and Yap2, with Yap1 activating the expression of *YCF1* and *GSH1* (Wemmie *et al.*, 1994; Wu and Moye-Rowley, 1994; Cohen *et al.*, 2002; Temple *et al.*, 2005).

Oxidative stress may be generated by toxic heavy metals, such as cadmium, but also by essential metals, such as iron, partly due to their ability to generate toxic hydroxyl radicals through the Fenton reaction (Halliwell and Gutteridge, 1984). There is growing evidence that iron deficiency may also lead to oxidative stress. In rats, iron deficiency has been shown to induce oxidative damage to the mitochondria and mitochondrial DNA (Walter *et al.*, 2002). Yeast, a strain lacking the iron-responsive transcriptional activators Aft1 and Aft2, both of which are required for the expression of genes involved in iron uptake, is hypersensitive to oxidative stress, and this sensitivity is decreased by the addition of iron to the growth medium (Blaiseau *et al.*, 2001). Yap1 has also been shown to up-regulate the expression of *AFT2* (Salin *et al.*, 2008). Finally, the redox status of the cell influences iron homeostasis: GSH depletion induces a specific defect in the maturation of cytoplasmic [Fe–S] proteins (Sipos *et al.*, 2002). Thus iron metabolism and thiol-dependent redox homeostasis are linked, and defects in one of these processes leads to an imbalance in the other.

Iron homeostasis and uptake are tightly regulated to prevent iron toxicity. Under aerobic conditions, iron is present mostly in its ferric form (Fe^{3+}) and is not available for use by the cell. *S. cerevisiae* uses two different systems to take up environmental iron: the reductive uptake mechanism and the siderophore transport system. The reductive system involves the reduction of ferric iron at the plasma membrane by reductases, followed by the uptake of ferrous iron by a high-affinity permease (Philpott, 2006). The nonreductive system involves iron uptake mediated by siderophores, small organic compounds that chelate ferric iron with high affinity. In *S. cerevisiae*, siderophore transport is mediated by four plasma membrane transporters of the major facilitator superfamily (MFS) of transporters (Goffeau *et al.*, 1997). Arn1 and Taf1/Arn2 are members of this family involved in the transport of ferrichromes (FCH) and triacetylfusarinine (TAF), respectively; Sit1/Arn3 transports ferrioxamine B (FOB) and ferrichrome (FCH); and Enb1/Arn4 transports enterobactin (ENB) (Lesuisse *et al.*, 1998, 2001; Heymann *et al.*, 1999, 2000a, 2000b; Yun *et al.*, 2000b). These four siderophore transporters belong to the Aft1 regulon (ARN) family and are regulated by the iron-responsive transcription factor Aft1 (Yun *et al.*, 2000a).

Phylogenetic analysis of the ARN family has revealed the existence of two uncharacterized homologues, *YCL073c* and *YKR106w* (Haas *et al.*, 2008), which we have named *GEX1* (glutathione exchanger) and *GEX2*, respectively. In this study, we show that Gex1 and Gex2 are mostly found at the vacuolar membrane. The production of Gex1 and Gex2 is induced under conditions of iron depletion and after H_2O_2 treatment, and Gex1 is regulated principally by Aft2. However, Gex1 and Gex2 are not involved in the transport of known siderophores. Instead, they are proton antiporters involved in glutathione exchange. Finally, we show that the deletion of *GEX1* and *GEX2* and the overexpression of *GEX1* modulate different signaling pathways (protein kinase A [PKA] and protein kinase C1 mitogen-activated protein kinase [PKC1-MAPK]), confirming a clear connection between iron, redox equilibrium, and the stress response.

RESULTS

Expression of the two paralogues *GEX1* and *GEX2* is regulated by iron depletion

S. cerevisiae expresses four siderophore transporters of the ARN family differing in substrate specificity (Haas *et al.*, 2008). These proteins are secondary transporters of the MFS subfamily (Philpott, 2006; Blaiseau *et al.*, 2010). Two other homologues of these ARN family genes, *YCL073c* and *YKR106w,* which we have named *GEX1* (glutathione exchanger) and *GEX2,* respectively, were not classified as ARN transporters because their expression was shown to be independent of Aft1 (Yun *et al.*, 2000a).

The amino acid sequences of Gex1 and Gex2 are 46% identical to that of their closest homologue, Arn1, and 33% identical to that of their most distant homologue, Enb1/Arn4. The amino acid sequences of Gex1 and Gex2 are 98% identical. Gex1 and Gex2 are predicted to have 12 transmembrane domains rather than the 14 generally observed in members of the ARN family of transporters. This is a common feature of MFS transporters (Pao *et al.*, 1998). No known protein motif was identified in sequence analyses with various prediction programs.

GEX1 and *GEX2* are present in the subtelomeric regions of chromosomes III and XI, respectively. This subtelomeric duplication is probably a recent divergence because the two fragments encode almost identical products (Gromadka *et al.*, 1996). Finally, the expression of *GEX1* and *GEX2* is undetectable in normal growth conditions (Gromadka *et al.*, 1996), and it has been suggested that this lack of expression may be due to the telomeric position of these genes, as genes close to the telomeres are generally silenced (Gottschling *et al.*, 1990). Given the high level of sequence identity between the coding sequences of *GEX1* and *GEX2,* it is impossible to distinguish the expression of one gene from that of the other. We therefore constructed strains bearing *GEX1* and *GEX2* tagged, at the chromosomal locus of the gene and at the carboxy terminus of the encoded protein, with different epitopes. Using the *GEX1-GFP/GEX2-HA* and *GEX1-HA/GEX2-GFP* strains grown under normal growth conditions (yeast extract peptone dextrose [YPD] or yeast nitrogen base [YNB]), we were unable to detect the expression of either of these genes, consistent with the findings of Gromadka *et al.* (1996) (Figure 1A). As *GEX1* and *GEX2* are homologous to members of the ARN family, we hypothesized that they might be induced under conditions of iron deficiency. We therefore cultured the same cells in the presence of bathophenanthroline bisulfonic acid (BPS), an iron chelator. We detected the expression of *GEX1* and *GEX2* after at least 16 h of growth in the presence of BPS (Figure 1A). The expression of *GEX2*, whether tagged with green fluorescent protein (GFP) or hemagglutinin (HA), was very weak, only about one-fourth that of *GEX1.*

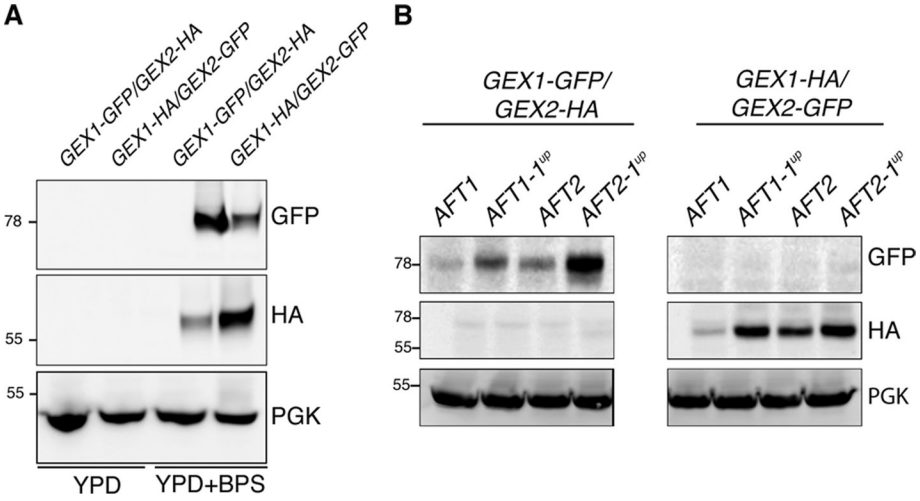

FIGURE 1: *GEX1* and *GEX2* are induced under conditions of iron depletion and Gex1 is regulated principally by Aft2. (A) *GEX1-GFP/GEX2-HA* or *GEX1-HA/GEX2-GFP* were grown in YPD or YPD supplemented with 200 μM BPS to midexponential growth phase. Total protein extracts were prepared and analyzed by Western immunoblotting with antibodies directed against GFP, HA, and phosphoglycerate kinase (PGK) as a loading control. (B) *GEX1-GFP/GEX2-HA* and *GEX1-HA/GEX2-GFP* cells carrying p*AFT1*, p*AFT1–1^{up}*, p*AFT2*, or p*AFT2–1^{up}* were grown overnight in YNB without doxycycline. Total yeast extracts were analyzed by Western immunoblotting for GFP, HA and PGK.

It has been shown that, unlike other members of the ARN family, *GEX1* and *GEX2* do not require Aft1 for their expression (Yun *et al.*, 2000a). We analyzed the promoter regions of *GEX1* and *GEX2* and found no Aft1 binding motif. However, we did identify an Aft2 binding motif, PuCACCC (Courel *et al.*, 2005), at −668 (ACACCC) in the promoter regions of the two genes. A second Aft2 binding motif was present only in the promoter region of *GEX1*, at −283 (ACACCC). For analysis of the regulation of *GEX1* and *GEX2* by Aft2 and Aft1, we constructed centromeric plasmids containing wild-type *AFT1* or *AFT2* or the constitutively active mutant alleles *AFT1–1^{up}* and *AFT2–1^{up}*. The four genes were placed under the control of the same promoter regulated by doxycycline. The plasmids were then introduced into the strains bearing tagged *GEX1* and *GEX2* genes, and protein extracts were analyzed by SDS–PAGE (Figure 1B). Under these experimental conditions, we were unable to detect *GEX2* expression. *GEX1*, whether tagged with HA or GFP, was induced more strongly by *AFT2* and *AFT2–1^{up}* than by *AFT1*and *AFT1–1^{up}*. The expression of *GEX1* in the presence of wild-type *AFT1* and *AFT2* expression showed that *GEX1* was a genuine target of these transcription factors, with *AFT2* more efficient than *AFT1*.

Gex1 is located at both the vacuolar and plasma membranes

We analyzed the distribution of Gex1 and Gex2 in strains with the corresponding genes tagged at the chromosomal locus (at the carboxy terminus of the encoded protein) with GFP or HA. The cells were grown to midexponential growth phase in the presence of BPS, and GFP fluorescence was analyzed by fluorescence microscopy (Figure 2, A and B). In the *GEX1-GFP* strain, fluorescence was detected at both the plasma and vacuolar membranes (Figure 2A). The distribution of the protein depended on the growth phase (Figure 2B). Very early in the exponential growth phase (optical density at 600 nm [OD_{600}] = 0.1) Gex1-GFP was present mostly at the plasma membrane, whereas in late exponential growth phase (OD_{600} = 3) this protein was found mostly at the vacuolar membrane. As shown by SDS–PAGE (Figure 1A), *GEX2-GFP* expression levels were much lower than those for *GEX1-GFP*, and the corresponding protein was barely detected. Like Gex1-GFP, Gex2-GFP was present at both the plasma and vacuolar membranes. Given the technical difficulty of detecting Gex2 production and the 98% identity of the two genes, we hypothesized that the two proteins were probably involved in the same process and decided to concentrate our studies on Gex1, except in genetic studies, in which we used a strain with a double deletion of *GEX1* and *GEX2*.

We tried to confirm the dual location of Gex1-HA by immunofluorescence studies, but we were unable to detect the protein by this approach (unpublished data). We then analyzed the distribution of the protein by sucrose gradient fractionation and Western immunoblotting on cells grown as in Figure 2A (Figure 2C). Gex1-GFP, which appeared to be located at the plasma and vacuolar membranes on the basis of GFP fluorescence, was present in fractions containing the plasma membrane ATPase Pma1 and internal fractions containing Vph1, the membrane subunit of the vacuolar ATPase. Some free GFP was detected in the soluble fraction (1–3), probably due to the endocytosis and degradation of Gex1-GFP in the vacuolar lumen (see later discussion and Supplemental Figure 2). For Gex1-HA, the protein was mostly found at the vacuolar membrane, as demonstrated by the cofractionation of Gex1-HA with Vph1 (Figure 2C). We hypothesized that Gex1-HA might, like Gex1-GFP, have a dual location, with most of the protein present at the vacuolar membrane and a smaller fraction present at the plasma membrane. We tested this hypothesis by tagging *GEX1* with HA at the chromosomal locus in the *end3*Δ mutant, which displays impaired internalization during endocytosis, ensuring that the plasma membrane was enriched in Gex1-HA. Gex1-HA, expressed in the *end3*Δ mutant, was detected in fractions colocalizing with the vacuolar membrane Vph1 but also in fractions colocalizing with the plasma membrane marker Pma1 (Figure 2C). Thus Gex1 presents a dual localization. The HA tag is smaller and is generally thought not to induce mislocalization. We therefore concluded that Gex1 was located mostly at the vacuolar membrane, with a smaller fraction of the protein present at the plasma membrane. The distribution of Gex1 depended both on the tag used and on expression levels. When Gex1 tagged with HA or GFP was overproduced under the control of a galactose promoter from a centromeric plasmid, Gex1-HA and Gex1-GFP were present at the plasma membrane, as shown by sucrose gradient fractionation and GFP fluorescence (Figure 2D).

Membrane-bound proteins are sorted in the trans-Golgi network (TGN) and are directed toward the plasma membrane or the vacuolar membrane. There are two alternative pathways for targeting membrane-bound proteins to the vacuole: the AP3 and VPS pathways. The AP3 pathway is a direct route, with vesicles originating from the Golgi apparatus directly fusing with the vacuole. The VPS pathway is an indirect pathway in which vesicles originating from the Golgi compartment fuse with late endosomes, which then fuse with the vacuole. We analyzed the targeting of Gex1-GFP to the vacuolar membrane with the *aps3*Δ mutant, which is affected in the AP3 pathway, and the *pep12*Δ mutant, affected in the fusion of Golgi-derived vesicles with late endosomes (Supplemental Figure 1). In

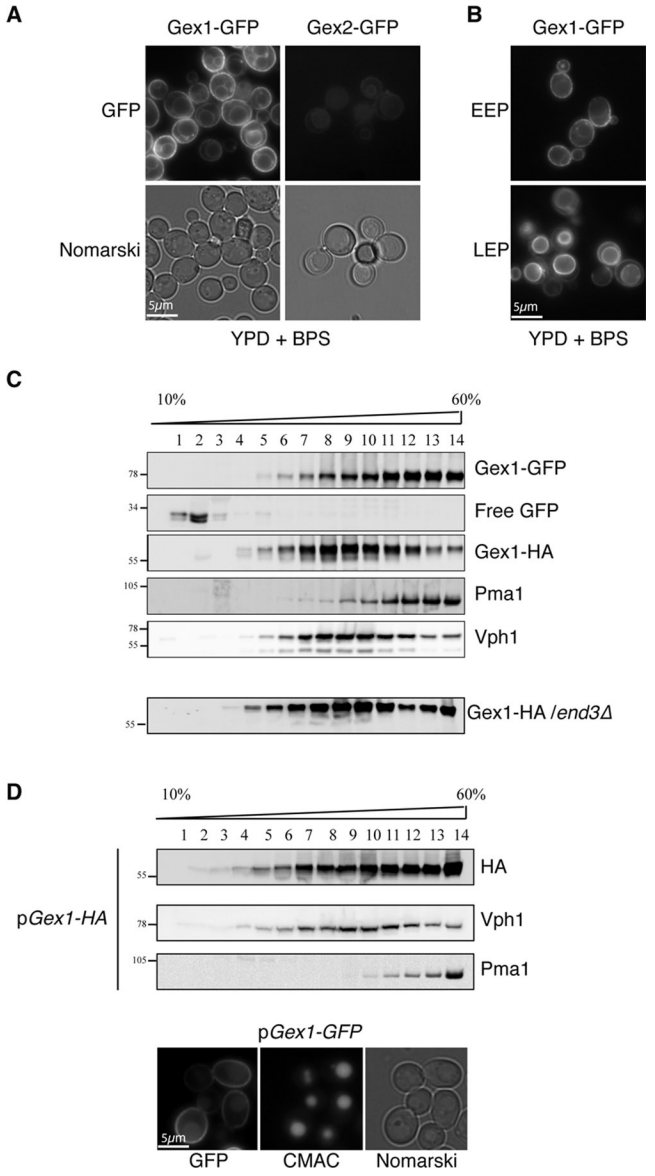

FIGURE 2: Subcellular localization of Gex1 and Gex2. *GEX1-GFP* and *GEX2-GFP* strains were grown overnight in YPD supplemented with 200 μM BPS and collected at midexponential growth phase (A) or very early in the exponential growth phase (EEP) (OD_{600} = 0.1) or in late exponential growth phase (LEP) (OD_{600} = 3) (B). GFP fluorescence was analyzed with the FITC filter set, and yeast morphology was studied with Nomarski optics. (C) *GEX1-GFP* or *GEX1-HA/end3*Δ cells were grown overnight in YPD supplemented with 200 μM BPS and collected at midexponential growth phase (as described in A). Cells were lysed and protein extracts were fractionated on a 20–60% sucrose density gradient. Aliquots of the various fractions were analyzed by Western immunoblotting for the presence of GFP, HA, plasma membrane ATPase 1 (Pma1), and transmembrane subunit of the vacuolar ATPase (Vph1). (D) Wild-type cells transformed with p*GEX1-HA* or p*GEX1-GFP* were grown overnight in YNB with 2% galactose. Protein extracts from the strain producing Gex1-HA were fractionated on a sucrose density gradient as described in C. Cells producing Gex1-GFP were treated with CMAC to stain the vacuolar lumen, and images of GFP (FITC filter set), CMAC (DAPI filter set), and cell shape (Nomarski optics) were taken.

the *aps3*Δ mutant, Gex1-GFP was detected at the vacuolar membrane, whereas in the *pep12*Δ mutant, Gex1-GFP was no longer targeted to the vacuolar membrane and the internal fraction of Gex1-GFP was trapped in vesicles. Thus Gex1-GFP is targeted to the vacuolar membrane via the VPS pathway.

Some Gex1-GFP was also present at the plasma membrane. Plasma membrane proteins that are no longer required undergo ubiquitylation, followed by endocytosis and targeting to the vacuole for degradation (Dupré *et al.*, 2004). We analyzed endocytosis of the plasma membrane–localized fraction of Gex1-GFP in the *GEX1-GFP* and *GEX1-GFP/pep4*Δ strains. In the *pep4*Δ strain, which lacks some vacuolar protease activities, protein degradation in the vacuole is delayed. The cells were cultured in the presence of BPS to very early in the exponential growth phase (OD_{600} = 0.1). In these growth conditions, Gex1-GFP was found principally at the plasma membrane (Supplemental Figure 2A). In the *GEX1-GFP/pep4*Δ strain, staining of the vacuolar lumen was observed at time 0, probably corresponding to the targeting of a small fraction of Gex1-GFP for degradation. Cells were washed and incubated in complete medium (YPD) without BPS for 2, 4, and 6 h. Gex1-GFP present at the plasma membrane at time 0 was progressively targeted for vacuolar degradation (after BPS chase) (Supplemental Figure 2, A and B). The vacuolar degradation of Gex1-GFP was delayed in the *GEX1-GFP/pep4*Δ strain, as shown by Western immunoblotting and fluorescence microscopy (accumulation of fluorescence in the lumen of the vacuole). Thus Gex1-GFP located at the plasma membrane underwent endocytosis when it was no longer required and was targeted to the vacuolar lumen for degradation.

GEX1 is a glutathione exchanger involved in oxidative stress response

The similarity of the sequences of *GEX1* and *GEX2* to those of other genes of the ARN family of siderophore transporters suggested a possible role for Gex1 and Gex2 in siderophore transport. We therefore measured the rate of iron uptake from various siderophores available in our laboratory in wild-type and *gex1*Δ *gex2*Δ strains: FOB, FCH, ENB, and TAF (Supplemental Figure 3A). No difference in the rate of uptake was observed between *gex1*Δ *gex2*Δ and wild-type strains for any of the siderophores studied, as suggested in a review by Winkelmann (2001). The presence of Gex1 at two different locations made this study more difficult. Thus, although no defect in iron uptake from siderophores was observed in the *gex1*Δ *gex2*Δ strain, we speculated that Gex1 might be involved in the vacuolar storage of intracellular siderophores. We then analyzed the intracellular distribution of internalized FOB in wild-type and mutant cells, using the gallium (GaIII) analogue of the fluorescent derivative of FOB, FOB-NBD (Froissard *et al.*, 2007) (Supplemental Figure 3B). Accumulation of the fluorescent probe in the vacuole was similar in mutant and wild-type cells (Supplemental Figure 3B). These results suggest that Gex1 and Gex2 are probably not involved in siderophore transport.

Gex1 and Gex2 belong to the MFS subfamily and may be involved in transporting metals other than iron. We therefore assessed the ability of the *gex1*Δ *gex2*Δ strain and of the strain overproducing Gex1 to grow on media containing high concentrations of divalent metals (Cd^{2+}, Ni^{2+}, Cu^{2+}, Mn^{2+}, Mg^{2+}, Co^{2+}, Zn^{2+}) and in the presence of the iron chelator BPS (Figure 3A and unpublished data). The *gex1*Δ *gex2*Δ mutant grew poorly only in the presence of the toxic heavy metal cadmium (Cd^{2+}). The strain overproducing Gex1-HA was more resistant to this metal than the wild-type strain transformed with an empty plasmid. We then quantified the cadmium, iron, and copper contents of cells grown in a Cd-supplemented medium (Figure 3B). No significant differences were found in the iron and copper contents of the various strains, whereas a clear difference between strains was observed for cadmium. The *gex1*Δ *gex2*Δ

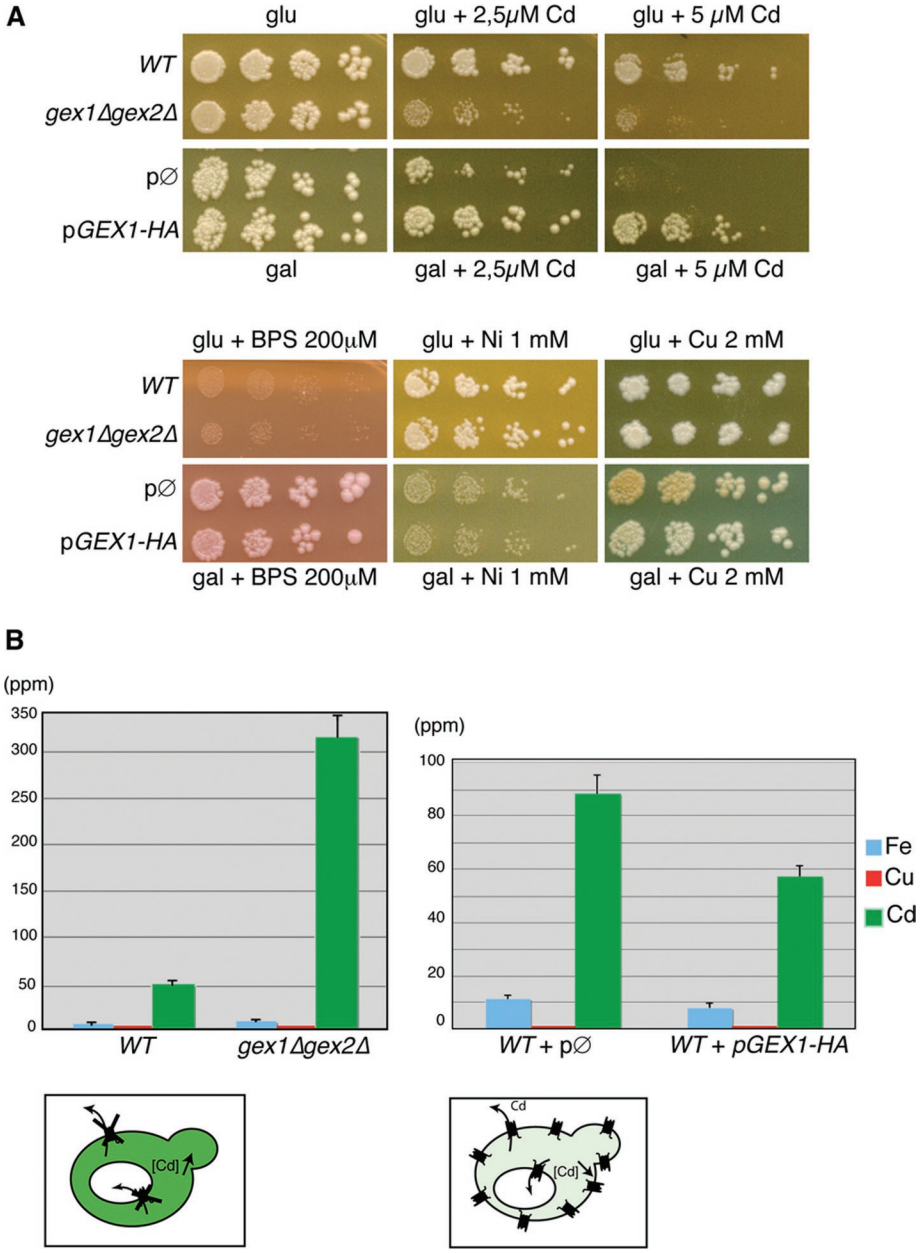

FIGURE 3: Gex1 and Gex2 are involved in cadmium uptake. (A) WT and *gex1*Δ *gex2*Δ cells were grown in YPD, subjected to serial fivefold dilution, and spotted onto solid glucose medium (glu) containing the indicated concentrations of cadmium ($CdSO_4$), BPS, nickel ($NiSO_4$), and copper ($CuSO_4$). The same experiment was carried out with WT cells transformed with the pØ or p*GEX1-HA* plasmids, except that cells were spotted onto complete galactose (gal)-containing medium. (B) WT and *gex1*Δ *gex2*Δ cells were grown in the presence of 1 μM cadmium for 6 h. WT cells bearing the pØ or p*GEX1-HA* plasmids were grown as in A, except that the carbon source was galactose instead of glucose. Iron, copper, and cadmium contents were then quantified for all strains by the inductively coupled plasma mass spectrometry method as carried out at the Service Central d'Analyse du CNRS (Solaize, France). The diagrams presented illustrate the consequence of *gex1gex2* deletions or Gex1 overproduction on cadmium content.

strain had a much higher cadmium content than wild-type cells, and the cells overproducing Gex1-HA had a lower intracellular cadmium content. Gex1-HA was targeted to the plasma membrane when overproduced from the p*GEX1-HA* plasmid (Figure 2D). A decrease in cadmium content may therefore be indicative of an increase in cadmium efflux at the plasma membrane mediated by Gex1-HA. These results are consistent with the growth phenotypes observed in the presence of cadmium, and they suggest that Gex1 may mediate cadmium export at the plasma membrane. The topology of membrane-bound proteins is acquired in the endoplasmic reticulum and remains constant, regardless of the final site to which the protein is targeted. Thus a protein with multiple membrane spans and amino and carboxy termini facing the cytosol will present the same topology at the plasma membrane and at the vacuolar membrane (schemes in Figure 3B). Gex1 at the vacuolar membrane may therefore mediate cadmium import into the vacuolar lumen and participate in cadmium detoxification.

In *S. cerevisiae*, cadmium detoxification is mediated principally by ATP-dependent glutathione S–conjugate pumps, which transport complexes of cadmium with glutathione from the cytosol to the extracellular medium or into the vacuolar lumen. We first analyzed total (reduced plus oxidized) and oxidized glutathione contents in the presence and absence of cadmium for the various strains (Figure 4).

Wild-type (WT) and *gex1*Δ *gex2*Δ strains grown in the absence of cadmium had redox ratios (GSH:GSSG) of 13:1 and 14:1, respectively, indicating that most of the intracellular free glutathione was present in a reduced form (Figure 4A). However, the *gex1*Δ *gex2*Δ strain had a higher intracellular glutathione content. After incubation of the cells with 1 μM cadmium, the total glutathione content of the *gex1*Δ *gex2*Δ strain was not significantly different from that of the wild-type strain, but the redox balance of the *gex1*Δ *gex2*Δ cells was shifted to the oxidized form of glutathione (GSSG), with a GSH:GSSG ratio of 5.5:1. In the *gex1*Δ *gex2*Δ strain, some reduced glutathione may have been associated with cadmium. This reduced glutathione accumulated in the cytosol of the cells, giving a ratio in favor of GSSG. The overproduction of Gex1-HA (which is known to be localized at the plasma membrane; see Figure 2D) resulted in a significantly lower total glutathione content than for the wild-type strain bearing an empty plasmid. This decrease was accompanied by an increase in the amount of the oxidized form of glutathione, giving a redox ratio of 3:1 (19:1 for the wild-type strain). No difference in total glutathione content was found between the strains bearing the empty plasmid or *pGEX1-HA* after exposure to cadmium, but the redox ratio favored oxidized glutathione when Gex1-HA was overproduced (GSH:GSSG of 3.5:1). Intracellular glutathione depletion or enrichment may be attributed to several factors (decrease/increase in biosynthesis, excretion, etc.). Gex1 is an MFS transporter that may be involved in transporting glutathione alone or in a complex with cadmium. We thus analyzed the excretion of glutathione into the medium in the presence and absence of cadmium for the

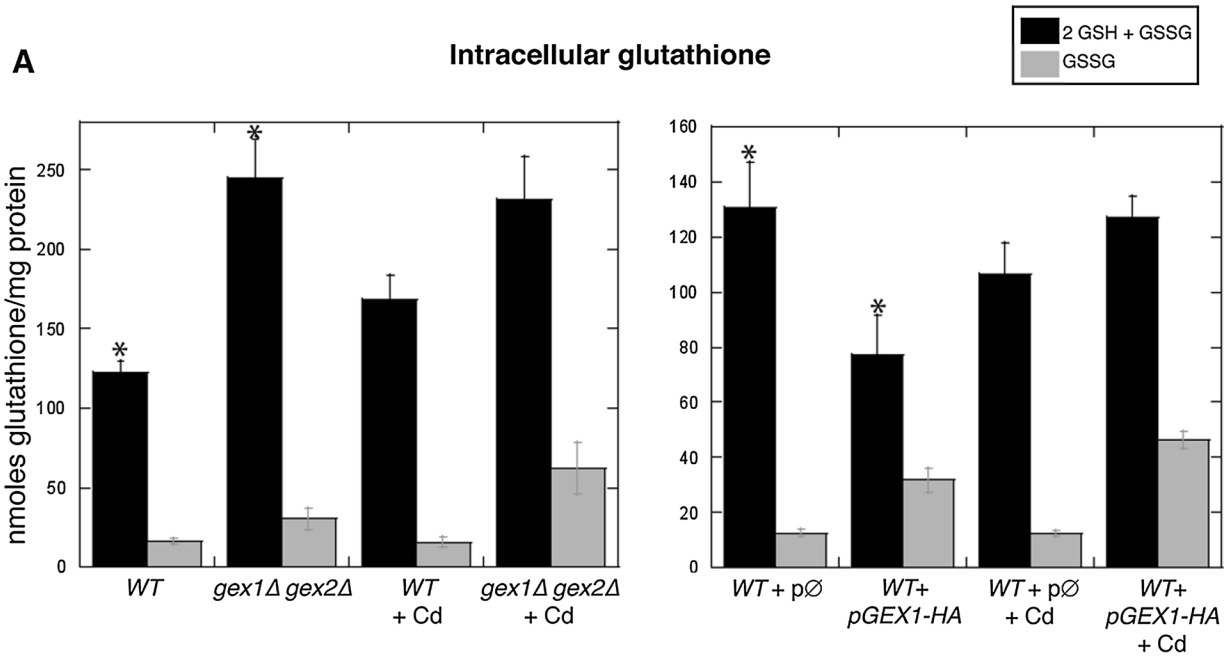

	GSH/GSSG
WT	13
gex1Δ gex2Δ	14
WT + Cd	19
gex1Δ gex2Δ + Cd	5.5
WT + pØ	19
WT + pGex1-HA	3
WT + pØ + Cd	15.5
WT + p*Gex1-HA* + Cd	3.5

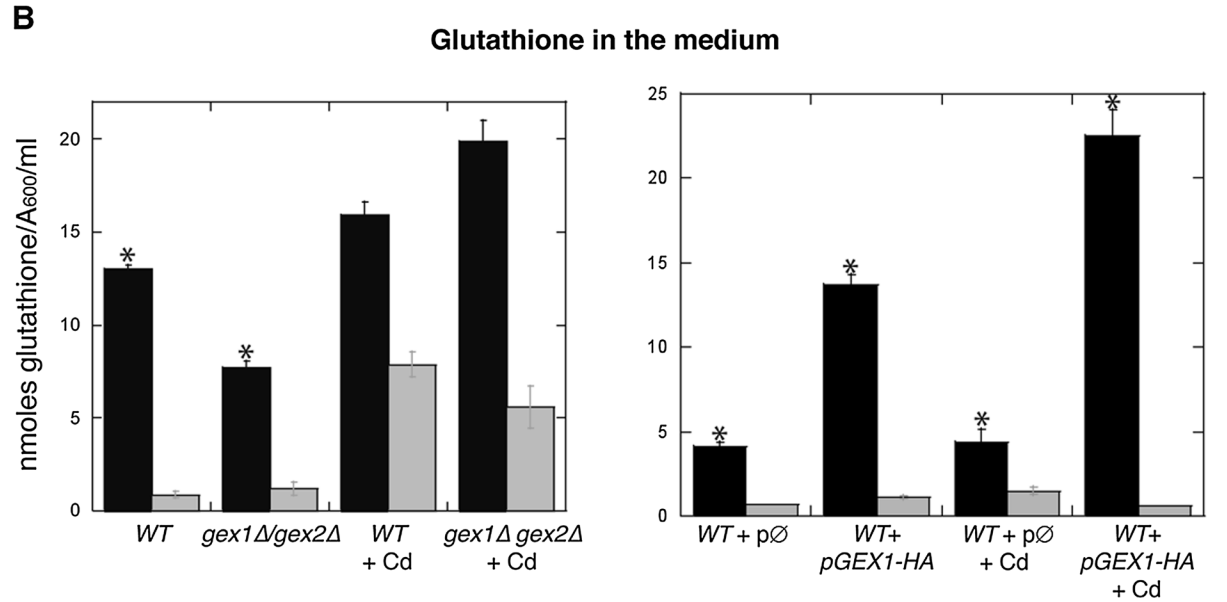

FIGURE 4: Glutathione distribution is dependent on *GEX1* and *GEX2* expression. WT, *gex1Δ gex2Δ*, WT + pØ, and WT + *pGEX1-HA* cells were grown in the presence or absence of 1 μM cadmium for 6 h (with galactose as a carbon source for the plasmid-bearing strains). The cells were centrifuged and total glutathione (reduced plus oxidized), and oxidized glutathione disulfide (GSSG) levels were determined in crude cell extracts (A) and in the medium (B) in the enzymatic recycling assay (see *Materials and Methods*). The values obtained were normalized with respect to protein content, determined in the BCA protein assay. The ratio GSH:GSSG for cell extracts is presented in the table (A). All data points in the figure represent means of at least six determinations. Asterisk indicates significant differences ($P < 0.005$, Student's *t* test).

various strains (Figure 4B). The *gex1*Δ *gex2*Δ cells excreted less glutathione into the medium than wild-type cells. In the presence of cadmium, there was no significant difference between the wild-type and *gex1*Δ *gex2*Δ strains. The two strains also presented similar amounts of oxidized glutathione in the medium. Cells overproducing Gex1-HA excreted more glutathione into the medium than the corresponding wild-type cells. Rates of excretion were five times higher than those of the wild-type strain in the presence of cadmium. Most of the glutathione excreted into the medium when Gex1-HA was overproduced was in the reduced form (GSH). Thus glutathione is excreted in its reduced form, probably as a complex with cadmium. GSH-Cd complexes are kinetically labile and dissociate rapidly in the extracellular medium, which has a lower cadmium concentration than the cells.

Low glutathione ratio (GSH:GSSG) may indicate that cells are subject to oxidative stress. We assessed the sensitivity of the various strains to oxidative stress generated by treatment with H_2O_2 (Figure 5A). We found that *gex1*Δ *gex2*Δ cells were hypersensitive to H_2O_2 and cells overproducing Gex1-HA were resistant to H_2O_2. This may indicate a role for Gex1 in protecting cells against exposure to H_2O_2. We analyzed Gex1-GFP levels after exposure to H_2O_2 and found that 40% of cells displayed faint GFP fluorescence after treatment with 0.1 mM H_2O_2 (Figure 5, B and C). Western immunoblotting analysis of Gex1-GFP levels after H_2O_2 treatment showed that H_2O_2 induced Gex1-GFP synthesis less efficiently than BPS treatment (levels after H_2O_2 treatment were only one-seventh those after BPS exposure). Finally, Gex1-GFP was not induced following overproduction of the transcription factors required for oxidative stress tolerance, Yap1 and Yap2 (Figure 5, B and C). Thus *GEX1* was involved in protecting cells against the oxidative stress induced by H_2O_2 treatment, and *GEX1* expression was not dependent on the stress-responsive factors Yap1 and Yap2 but may have been dependent on the iron-responsive transcription factor Aft2.

Gex1 and Gex2 are proton H^+ antiporters

Gex1 and Gex2 are members of the MFS family of transporters and are therefore predicted to be proton antiporters or symporters (Goffeau *et al.*, 1997). We assessed the ability of Gex1 to mediate proton exchange by analyzing the cytosolic pH of the *gex1*Δ *gex2*Δ strain and of the strain overproducing Gex1-HA, using a GFP variant, the ratiometric pHluorin, which is sensitive to pH (Miesenböck *et al.*, 1998; Dechant *et al.*, 2010) (Figure 6A). As control strains, we used the *nha1*Δ and *nhx1*Δ mutants, which have a higher and lower pH, respectively, than the wild-type strain (Sychrova *et al.*, 1999; Brett *et al.*, 2005). The ratiometric pHluorin variant was found in the cytosol and nucleus but was excluded from the vacuole. The *gex1*Δ *gex2*Δ cells displayed lower levels of cytosolic fluorescence, indicative of a cytosolic pH higher than that of the wild-type strain but lower than that of the *nha1*Δ mutant. The cells overproducing Gex1-HA (which was localized at the plasma membrane) displayed a higher level of cytosolic fluorescence than the wild-type strain (but lower than that of the *nhx1*Δ mutant), indicating acidification of the cytosol and thus the import of H^+ ions into the cytosol, probably mediated by Gex1-HA. This acidification of the cytosol was responsible for the extensive vacuole fragmentation observed when Gex1-HA was overproduced (Supplemental Figure 4).

We further confirmed the results obtained by the quantitative analysis of fluorescence. The ratio of fluorescence at 508 nm in response to excitation at two different wavelengths (I_{410}/I_{470}) was proportional to cytosolic pH (Miesenböck *et al.*, 1998; Brett *et al.*, 2005). The ratios obtained confirmed our fluorescence observations.

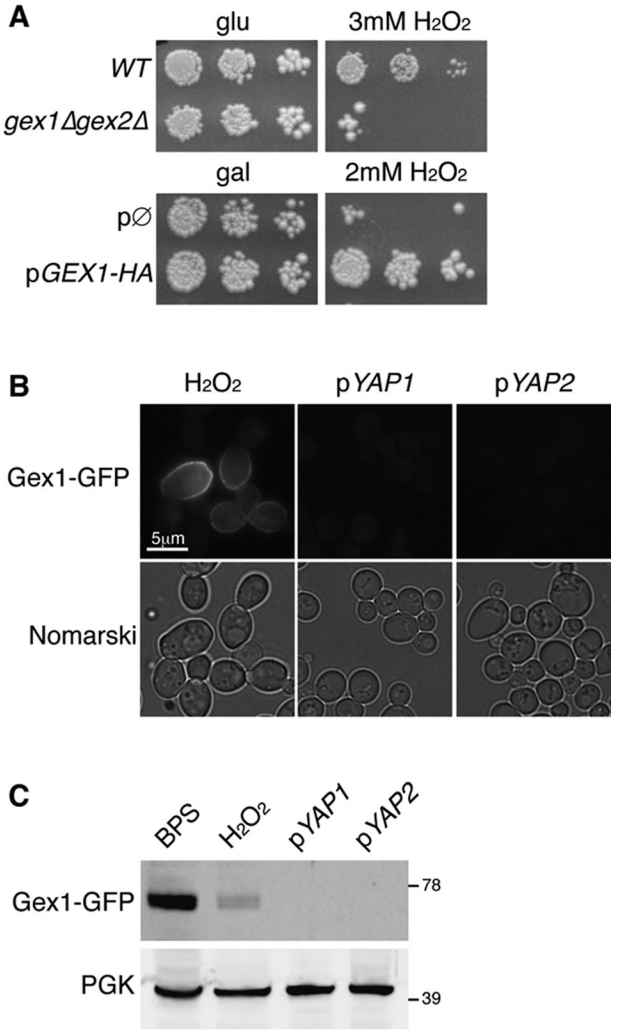

FIGURE 5: Gex1 and Gex2 are involved in the oxidative stress response. (A) WT and *gex1*Δ *gex2*Δ cells were spotted onto solid glucose medium (glu) containing the indicated concentrations of H_2O_2. This experiment was repeated with wild-type cells (WT) bearing the pØ or p*GEX1-HA* plasmids, except that the cells were spotted onto galactose (gal)-containing plates. (B) *GEX1-GFP* cells were cultured overnight in YPD containing H_2O_2 (0.1 mM). *GEX1-GFP* cells transformed with p*YAP1* and p*YAP2* were grown overnight in YNB supplemented with glucose as a carbon source. GFP fluorescence was visualized with the FITC filter set, and cell shape was studied with Nomarski optics. (C) Total protein extracts from the same cells as in B and *GEX1-GFP* cells grown overnight in YPD supplemented with 200 μM BPS were prepared and analyzed by Western immunoblotting with antibodies directed against GFP and PGK as a loading control.

A change in cytosolic pH might also lead to a change in the pH of the vacuole. We therefore assessed vacuolar acidity, using the intracellular pH indicator quinacrine (Baggett *et al.*, 2003) (Figure 6C). No detectable difference in vacuolar quinacrine staining was observed between the wild-type and *gex1*Δ *gex2*Δ mutant cells. By contrast, the overproduction of Gex1-HA resulted in more intense quinacrine staining, indicative of vacuole acidification. This acidification of the vacuole was probably an indirect effect of the cytosol acidification mediated by the Gex1-HA at the plasma membrane, as shown for other mutants, including *nhx1*Δ (Brett *et al.*, 2005).

Hence these experiments indicate that Gex1 is a proton antiporter that makes use of the proton motive force at the plasma and

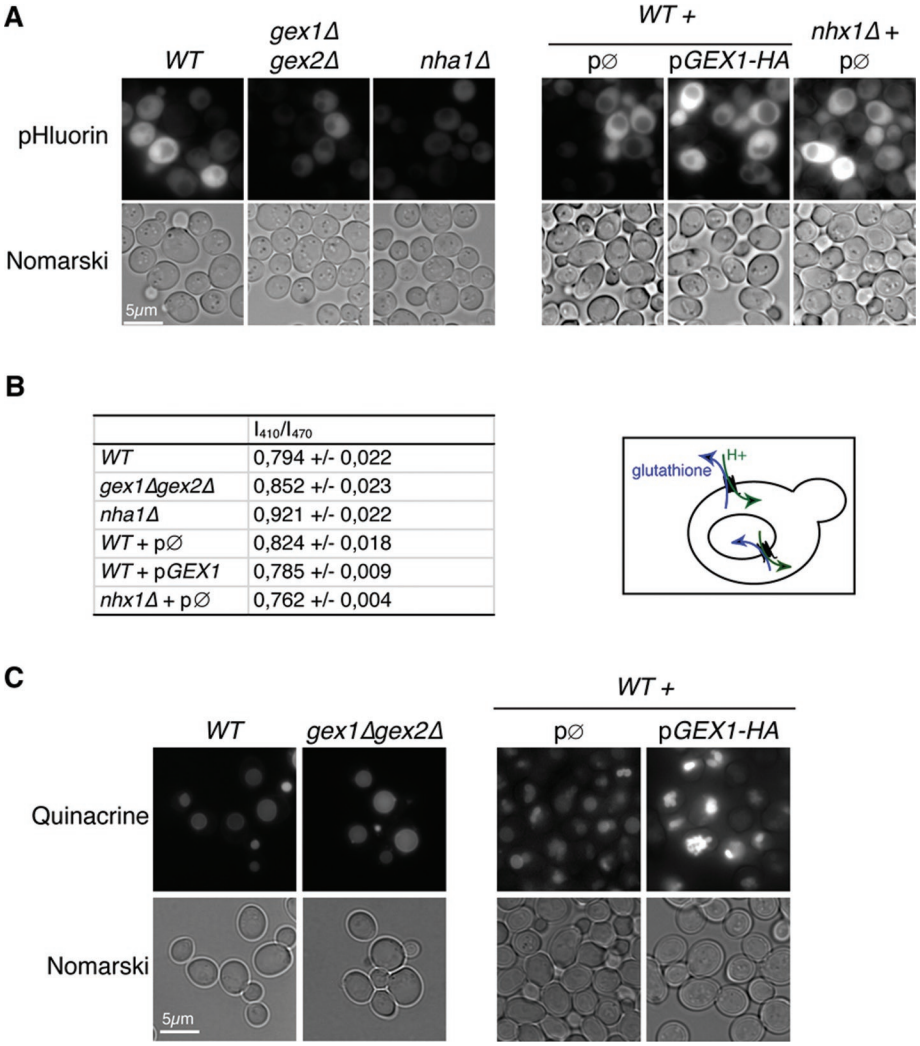

	I_{410}/I_{470}
WT	0,794 +/- 0,022
gex1Δgex2Δ	0,852 +/- 0,023
nha1Δ	0,921 +/- 0,022
WT + p*Ø*	0,824 +/- 0,018
WT + p*GEX1*	0,785 +/- 0,009
nhx1Δ + p*Ø*	0,762 +/- 0,004

FIGURE 6: The overproduction of Gex1-HA induces acidification of the cytosol and the vacuole. (A) WT, *gex1*Δ *gex2*Δ, and *nha1*Δ cells transformed with p*ADH1-pHluorin* were grown overnight to midexponential growth phase in glucose-containing medium. WT cells cotransformed with p*ADH1-pHluorin* and the pØ or the p*GEX1-HA* plasmids and *nhx1*Δ cells cotransformed with p*ADH1-pHluorin* and pØ plasmids were grown to midexponential phase in galactose-containing medium. Fluorescence was visualized with the FITC filter set (characteristics given in *Materials and Methods*), and cell shape was studied with Nomarski optics. (B) Fluorescence intensity values (arbitrary units) were obtained for an emission wavelength of 508 nm for two excitation wavelengths: 410 and 470 nm (I_{410} and I_{470}) (the values correspond to at least 70 measurements). (C) WT and *gex1*Δ *gex2*Δ cells were grown in YPD. WT cells transformed with the pØ or p*GEX1-HA* plasmids were grown overnight in galactose-containing medium. All strains were stained with quinacrine, analyzed for quinacrine fluorescence, and studied with Nomarski optics. The diagram illustrates a proposed mode of action for Gex1-HA.

vacuolar membranes to mediate glutathione exchange (scheme in Figure 6).

Gex1 and Gex2 contribute to modulation of the PKA and PKC1-MAPK signaling pathways

Dechant *et al.* (2010) recently demonstrated that cytosolic pH regulates the PKA glucose signaling pathway and a genome-wide screen for mutants overexcreting glutathione identified mutants of the PKA pathway as having the highest levels of glutathione excretion (22–25 times higher than that of wild-type cells; Perrone *et al.*, 2005). We showed that Gex1-HA overproduction induced acidification of the cytosol and a decrease in glutathione content. We therefore investigated the possible role of Gex1 and Gex2 in the PKA pathway. For this purpose, we transformed the *gex1*Δ *gex2*Δ deletion mutant and the strain overproducing Gex1-HA with a plasmid encoding the stress-responsive transcription factor Msn2 tagged with GFP (Görner *et al.*, 1998). Msn2 is targeted to the nucleus in response to various stresses, including oxidative stress and acidification of the cytosol, through the action of several signaling cascades, including the PKA pathway. The disruption of *GEX1* and *GEX2* induced a defect in the targeting of Msn2-GFP to the nucleus, and Gex1-HA overproduction induced a relocalization of Msn2-GFP to the nucleus, consistent with the induction by Gex1-HA of cytosol acidification (Figure 7A). Msn2 and Msn4 have been shown to increase the expression of genes involved in glycogen synthesis (Smith *et al.*, 1998). Thus defects in Msn2 targeting to the nucleus lead to a decrease in glycogen accumulation. We assessed glycogen accumulation in the cells, using an iodine solution (Figure 7B). The disruption of *GEX1* and *GEX2* resulted in lower glycogen content than for the wild-type strain, confirming a defect in the targeting of Msn2 to the nucleus. The wild-type strain transformed with an empty plasmid behaved like the wild-type strain transformed with p*GEX1-HA* because glycogen is hardly synthesized when cells are grown on galactose as the sole carbon source.

We assessed Msn2 activation in cells overproducing Gex1-HA by searching for targets of Msn2 potentially involved in oxidative stress. The PKC1-MAPK pathway is essential for cell survival in conditions of oxidative stress (Vilella *et al.*, 2005). Activation of the PKC1-MAPK pathway leads to activation of Slt2/Mpk1, the last member of this cascade. Mpk1 is activated by phosphorylation, and strict timing of the phosphorylation/dephosphorylation of Mpk1 is essential for cell survival. Two phosphatases are involved in the dephosphorylation of Mpk1: Sdp1 and Msg5. Sdp1 is specific for Mpk1, and its expression is induced by Msn2 in conditions of oxidative stress (reviewed in Martín *et al.*, 2005). We therefore analyzed the phosphorylation profile of Slt2/Mpk1 in the *gex1*Δ *gex2*Δ mutant strain and in a wild-type strain (Figure 7C). The phosphorylation of Mpk1 was not affected in the *gex1*Δ *gex2*Δ strain, consistent with the cytosolic location of Msn2. We further analyzed the phosphorylation of Mpk1 in WT, *MPK1-GFP*, and *sdp1*Δ strains with and without Gex1-HA overproduction. The overproduction of Gex1-HA had no effect on Mpk1-GFP levels but induced the dephosphorylation of Mpk1, whether untagged or tagged with GFP (Figure 7C). In the strain lacking *SDP1*, the dephosphorylation of Mpk1 was abolished, and Mpk1 phosphorylation levels were even higher than those in a strain bearing an empty plasmid. We also carried out a more general analysis of the MAP kinase pathway, using calcofluor white (CFW), a chitin

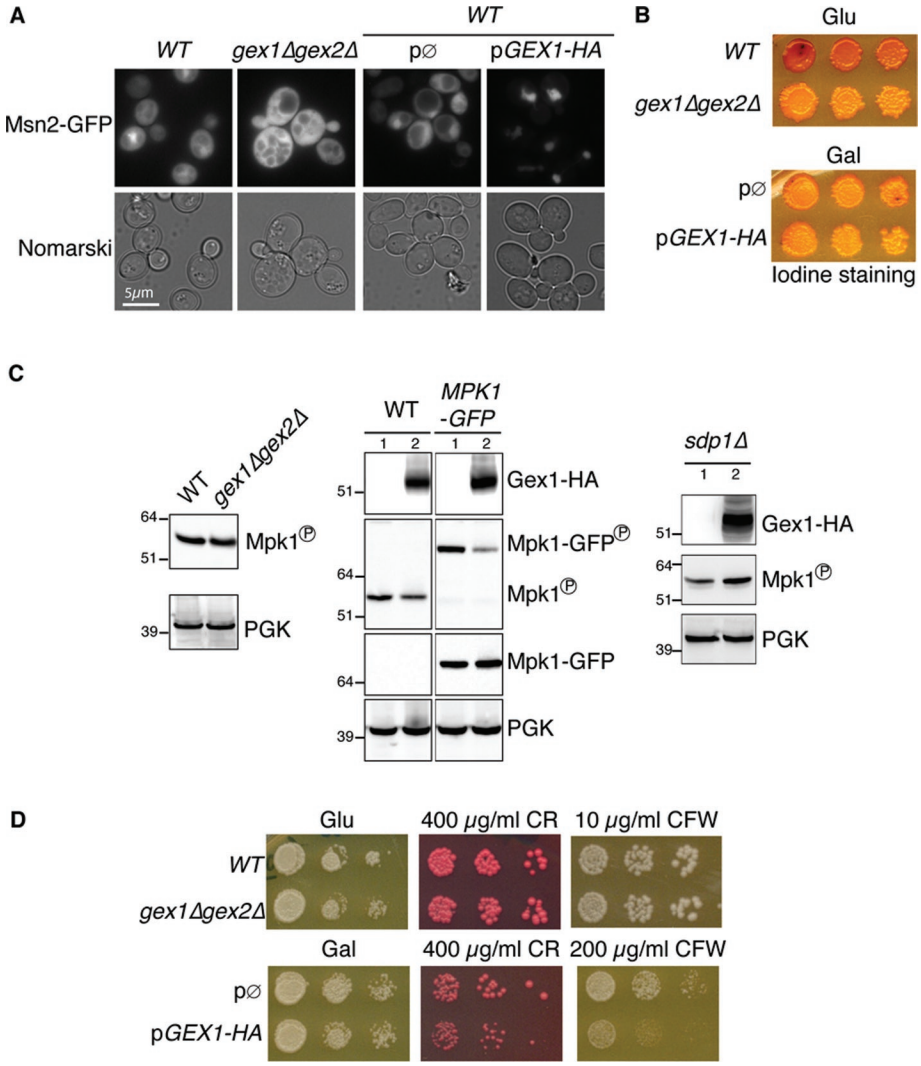

FIGURE 7: Influence of *GEX1* and *GEX2* on the PKA and MAPK pathways. (A) WT cells transformed with p*ADH1-MSN2-GFP* alone or in combination with the pØ or p*GEX1-HA* plasmids, and *gex1*Δ *gex2*Δ cells transformed with p*ADH1-MSN2-GFP*, were grown overnight to midexponential growth phase. Slides were exposed only once to ensure that Msn2-GFP was not targeted to the nucleus due to light exposure. (B) WT and *gex1*Δ *gex2*Δ cells and WT cells transformed with the pØ or p*GEX1-HA* plasmid were sequentially diluted fivefold and spotted onto glucose-containing medium for *WT* and *gex1*Δ *gex2*Δ and onto galactose-containing medium for the other strains. Plates were incubated for 3 d, and glycogen accumulation was assayed by gently pouring an iodine solution over the spots. (C) WT, *gex1*Δ *gex2*Δ, and cells transformed with the pØ (1) and p*GEX1-HA* (2) plasmids were grown overnight in glucose-containing or galactose-containing (for strains bearing plasmids) medium, and extracts of the cells were prepared and subjected to Western immunoblotting. Gex1-HA was detected with a monoclonal anti-HA antibody, Mpk1-GFP was detected with a monoclonal anti-GFP antibody, and the phosphorylated forms of Mpk1 were detected with a polyclonal anti–phospho-p44/42 MAPK antibody. PGK was detected with a polyclonal antibody and was used as a loading control. (D) The cells described in B were subjected to fivefold dilution and spotted onto glucose- or galactose-containing medium with the indicated concentrations of cell wall–stressing agents Congo red (CR) and calcofluor white (CFW).

antagonist that interferes with cell wall assembly, and the cell wall–stressing 1,3-glucan–binding dye Congo red (CR) (Figure 7D). We observed no difference in the growth rates of the wild-type and *gex1*Δ *gex2*Δ mutant strains, whereas the overproduction of Gex1-HA rendered wild-type cells sensitive when cultured on plates in the presence of CFW or CR, confirming inhibition of the cell wall integrity pathway response (Chen *et al.*, 2005; Lesage *et al.*, 2005). Our results thus indicate that Gex1 and, probably, Gex2 affect the PKA and PKC1-MAPK signaling pathways by disturbing the pH and thiol-redox homeostasis of the cells.

DISCUSSION

GEX1 and *GEX2* expression

GEX1 and *GEX2* are paralogues, presenting 98% sequence identity and mapping to the subtelomeric regions of two different chromosomes (Gromadka *et al.*, 1996). The other *S. cerevisiae* homologues of *GEX1* and *GEX2, ARN1–4,* also map to subtelomeric regions but are farther from the end of the chromosome than *GEX1* or *GEX2*. It has been suggested that the subtelomeric region of the chromosome is a reservoir of silenced genes involved in adaptive responses (Fabre *et al.*, 2005). We found that *GEX1* and *GEX2* were expressed only under certain growth conditions in which the cells were subject to stress. However, despite the lack of detection of Gex1 or Gex2 by Western immunoblotting or fluorescence, the *gex1*Δ *gex2*Δ double deletant was sensitive to cadmium and H_2O_2 and was affected in terms of its cytosolic pH and glutathione homeostasis, consistent with the presence of Gex1 and/or Gex2 but in amounts too small to be detected.

GEX1 and *GEX2* are induced under conditions of iron depletion, as expected for genes homologous to those of the ARN family of siderophore transporters. Unlike other members of the ARN family, *GEX1* is induced principally by the iron-responsive transcriptional factor Aft2 and, to a lesser extent, by its paralogue Aft1. Gex1 has two specific Aft2 binding motifs in its promoter region, at −283 and −668. Only one Aft2 binding site, the farthest from the ATG codon, is present in the promoter region of *GEX2*. This may account for the lack of *GEX2* expression in conditions of Aft2 and Aft2–1^{up} production. Another element that could account for the lack of *GEX2* expression in conditions of iron depletion is the location of *GEX2*, closer to the telomere than *GEX1*, potentially enhancing the silencing of *GEX2*. Silencing close to the telomeres is probably the principal system of regulation for *GEX1* and *GEX2* because the reduction of nucleosome content by the histone H4 depletion increases the expression of *GEX1* and *GEX2* (Wyrick *et al.*, 1999).

There are very few examples of genes regulated principally by Aft2. Such genes include those encoding the divalent metal ion vacuolar transporter Smf3, the mitochondrial iron transporter Mrs4, and the mitochondrial iron–sulfur cluster assembly Isu1 (Rutherford *et al.*, 2001; Courel *et al.*, 2005). However, all these studies have reported a role for Aft2 in gene transcription only in the absence of *AFT1* or in the *AFT2–1*^{up} gain-of-function mutant (Rutherford *et al.*, 2001; Courel *et al.*, 2005). *GEX1* is the first example of a gene clearly

regulated by Aft2 in a wild-type genetic context. Our results are also consistent with the hypothesis that Aft2 is involved principally in the regulation of proteins involved in vacuolar and mitochondrial transport (Courel *et al.*, 2005).

We also found that *GEX1* was induced under H_2O_2 treatment and that this induction was independent of the redox-responsive YAP regulon (*YAP1* and *YAP2*). Previous studies have shown that the *aft1*Δ *aft2*Δ double mutant presents a number of phenotypes related to oxidative stress, including H_2O_2 hypersensitivity. It has been suggested that *AFT1* and *AFT2* have overlapping functions in iron homeostasis and oxidative stress resistance, and *AFT2* has been shown to be directly regulated by *YAP1* (Blaiseau *et al.*, 2001; Salin *et al.*, 2008). Gex1 was induced after treatment with the iron chelator BPS, and iron depletion is known to induce oxidative stress. Thus *GEX1* expression is probably due to oxidative stress and not directly linked to iron transport. Our study suggests that Aft2 regulates Gex1 induction under oxidative stress conditions in a Yap1-independent manner.

Gex1 is located at two sites within the cell

The location of Gex1 at two sites—the plasma membrane and the vacuolar membrane—is very unusual but not unique. A few other examples of yeast proteins located at several sites in the steady state are known. One such example is the chloride channel Gef1, a member of the voltage-activated Cl^- channel group (Greene *et al.*, 1993). Gef1 has been shown to function at the Golgi apparatus, vacuolar membrane, and plasma membrane (Gaxiola *et al.*, 1998; Schwappach *et al.*, 1998; Lopez-Rodriguez *et al.*, 2007). The presence of Gef1 at multiple sites is important for the maintenance of normal Cl^- homeostasis in the cell. In mammalian cells, the lysosomal transporter LYAAT-1/PAT1, an H^+/amino acid symporter, is located at the lysosomal/vacuolar membrane in neurons and is involved in the efflux of amino acids from the lysosome (Sagne *et al.*, 2001). By contrast, in gut cells, this transporter is located at the plasma membrane, where it functions in the absorption of amino acids (Boll *et al.*, 2004).

The mechanisms involved in the dual targeting of Gex1 to the plasma and vacuolar membranes remain to be elucidated. Transmembrane proteins following the secretory pathway are sorted in the TGN, within which they may be targeted to the plasma membrane or to the multivesicular bodies (MVBs) and hence to the vacuole. Two main signals are involved in targeting proteins to the MVBs: peptide motifs present in the cytosolic domains of the proteins are involved in exit from the TGN, and the ubiquitylation of cytosolic lysine residues is responsible for the targeting to the MVBs of membrane proteins originating from the plasma membrane or the TGN (Bonifacino and Traub, 2003; Lauwers *et al.*, 2010).

We found that Gex1 was down-regulated in the absence of BPS in the culture medium. Ubiquitin is the only signal known to induce the internalization of plasma membrane transporters in yeast, and Rsp5 has been shown to be the only ubiquitin ligase involved in the internalization of all plasma membrane transporters in yeast. Thus Gex1 from the plasma membrane is probably ubiquitylated in an Rsp5-dependent manner before being targeted to the MVBs and the vacuolar lumen. Gex1 targeted from the TGN to the vacuole via the VPS pathway was probably not ubiquitylated because it was localized at the membrane and was not present within the lumen of the vacuole. It remains unclear how this is achieved. Are there different signals involved in the targeting of Gex1 to the vacuole depending on whether it comes from the TGN or from the plasma membrane? Are there different ubiquitylation–deubiquitylation events mediating this regulation? Does the trafficking of Gex1 depend on the concentration of its substrates? It has been shown for the uracil permease Fur4 and for the divalent metal ion transporter Smf1 that the availability and/or concentration of the substrate may cause a change in the conformation of the protein on its way to the plasma membrane, resulting in direct targeting to the vacuole rather than to the plasma membrane (Liu and Culotta, 1999; Blondel *et al.*, 2004). A similar hypothesis could be proposed for Gex1. Gex1 cotransports glutathione and H^+. We have shown that BPS, and thus probably oxidative stress, induces the production of Gex1 and Gex2 only after 16 h of growth. Yeast is known to acidify the culture medium, and, after 16 h of growth, the two substrates of Gex1 are present: glutathione within the cells and H^+ outside the cells. Early in the exponential growth phase, Gex1 is present mostly at the plasma membrane and mediates cytosol acidification and the extrusion of glutathione. The low pH of the cytosol induces acidification of the yeast vacuole, probably inducing the targeting of Gex1 from the TGN to the vacuolar membrane, where it can import glutathione and export H^+ out of the vacuolar lumen. Thus the production and location of Gex1 probably depend on the presence of its two substrates. The molecular mechanisms involved in the routing of Gex1 remain to be deciphered.

GEX1 is a proton antiporter for glutathione

The results of this study demonstrate that Gex1 is involved in the exchange of glutathione, a strong antioxidant and a powerful detoxifying tripeptide. We also show that Gex1 functions as a proton/glutathione antiporter. At the vacuolar membrane, H^+ is exported into the cytosol and glutathione is imported through the vacuolar membrane. At the plasma membrane, H^+ is imported into the cytosol and glutathione is exported to the extracellular medium. This export facilitates cadmium detoxification when cells are grown in the presence of this metal. However, glutathione is transported even in the absence of cadmium, indicating that the cadmium–glutathione complex is probably not the primary substrate of Gex1 and that Gex1 could probably transport glutathione coupled to another divalent cations.

Gex1 and Gex2 are homologous to the members of the siderophore transporter family ARN1–4. Surprisingly, the deletion of the *GEX1* and *GEX2* genes had no effect on iron uptake from different siderophores. Ferrichrome, the substrate of Arn1, is a cyclical hexapeptide (Philpott *et al.*, 2002). Glutathione is a tripeptide, but two molecules of glutathione are required for the interaction with cadmium (Belcastro *et al.*, 2009). The structures of glutathione and ferrichrome are similar, and transporters presenting sequence similarities could transport molecules with similar structures. Furthermore, sequence similarity does not inevitably lead to the transport of the same molecules. A good example of this is provided by the multidrug resistance and pleiotropic drug resistance families of transporters, which have similar sequences but transport a broad range of molecules of different categories (for review see Jungwirth and Kuchler, 2006; Panwar *et al.*, 2008).

Gex1 and signaling

GEX1 is induced under stress conditions, such as iron depletion or H_2O_2 exposure. We have shown that the disruption of *GEX1* and *GEX2* or the overproduction or Gex1 leads to changes in the cytosolic pH and glutathione content of cells. These two phenomena are tightly regulated by the cells and involve different signaling pathways and different transcription factors. Msn2 is a stress response transcriptional activator involved in regulating almost 200 genes (involved in response to heat shock, osmotic shock, oxidative stress, low pH, glucose starvation, etc.) and is a target of the

Strain	Genotype	Source/reference
WT (BY4741)	*Mat a his3Δ1 leu2Δ0 met15Δ0 ura3Δ0*	EUROSCARF
WT HIS$^+$ (BY4741 HIS$^+$)	*Mat a HIS3$^+$ leu2Δ0 met15Δ0 ura3Δ0*	This study
BY4742 (WT)	*Mat alpha his3Δ1 leu2Δ0 lys2Δ0 ura3Δ0*	EUROSCARF
WT HIS$^+$ (BY4742 HIS$^+$)	*Mat alpha HIS3$^+$ leu2Δ0 lys2Δ0 ura3Δ0*	This study
GEX1-GFP/GEX2-HA (NBT 523)	*Mat a his3Δ1 leu2Δ0 met15Δ0 ura3Δ0 GEX1-GFP::HIS3MX6, GEX2–6HA::KANMX6*	EUROSCARF
GEX1-HA/GEX2-GFP (NBT 526)	*Mat a his3Δ1 leu2Δ0 met15Δ0 ura3Δ0 GEX2-GFP::HIS3MX6 GEX1–6HA::KANMX6*	This study
GEX1-HA (NBT584)	*Mat a his3Δ1 leu2Δ0 met15Δ0 ura3Δ0 GEX1–6HA::HIS3MX6*	This study
GEX2-HA (NBT583)	*Mat a his3Δ1 leu2Δ0 met15Δ0 ura3Δ0 GEX2–6HA::HIS3MX6*	This study
GEX1-GFP (NBT 513)	*Mat a his3Δ1 leu2Δ0 met15Δ0 ura3Δ0 GEX1-GFP::HISMX6*	This study
GEX1-GFP/pep4Δ (NBT 608)	*Mat a his3Δ1 leu2Δ0 met15Δ0 ura3Δ0 GEX1-GFP::HISMX6 pep4Δ::KANMX6*	This study
GEX2-GFP (NBT516)	*Mat a his3Δ1 leu2Δ0 met15Δ0 ura3Δ0 GEX2-GFP::HISMX6*	This study
gex1Δ gex2Δ (NBT 472)	*Mat alpha his3Δ1; leu2Δ0; lys2Δ0; ura3Δ0; gex2::HIS; gex1::KanMX6*	This study
GEX1-GFP/aps3Δ (NBT 537)	*Mat a his3Δ1 leu2Δ0 met15Δ0 ura3Δ0 aps3::KanMX6 GEX1-GFP::HIS3MX6*	This study
GEX1-GFP/pep12Δ (NBT 535)	*Mat a his3Δ1 leu2Δ0 met15Δ0 ura3Δ0 pep12::KanMX6 GEX1-GFP::HIS3MX6*	This study
VMA5-GFP	*Mat a his3Δ1 leu2Δ0 met15Δ0 ura3Δ0 VMA5-GFP::HIS3MX6*	Invitrogen
MPK1-GFP	*Mat a his3Δ1 leu2Δ0 met15Δ0 ura3Δ0 MPK1-GFP::HIS3MX6*	Invitrogen
sdp1Δ	*Mat a his3Δ1 leu2Δ0 met15Δ0 ura3Δ0 sdp1::KanMX6*	EUROSCARF
nhx1Δ	*Mat a his3Δ1 leu2Δ0 met15Δ0 ura3Δ0 nhx1::KanMX6*	EUROSCARF
nha1Δ	*Mat a his3Δ1 leu2Δ0 met15Δ0 ura3Δ0 nha1::KanMX6*	EUROSCARF

EUROSCARF, European *Saccharomyces cerevisiae* Archive for Functional Analysis, Institute of Molecular Biosciences, Johann Wolfgang Goethe-University Frankfurt, Frankfurt, Germany.

TABLE 1: *S. cerevisiae* strains.

PKA and PKC1-MAPK signaling pathways. It was thus a perfect candidate for involvement in the response to pH and redox imbalance observed when Gex1 is overproduced or when *GEX1* and *GEX2* are disrupted. We showed that Msn2 was present mostly in the cytosol when *GEX1* and *GEX2* were disrupted and was targeted to the nucleus when Gex1 was overproduced. The PKA pathway was affected in the *gex1Δ gex2Δ* strain, and this defect was probably due to alkalinization of the cytosol. Down-regulation of the PKC1-MAPK pathway was impaired in the strain overproducing Gex1 due to the action of the Sdp1 phosphatase on Mpk1/Slt2. The down-regulation of the PKC1-MAPK pathway after Gex1-HA overproduction is probably not a direct consequence of the production of the protein itself, instead resulting from changes in the redox status of the cells (GSH:GSSG ratio of 3:1). We have shown that Gex1-HA is induced by H_2O_2. Thus overproducing a protein induced by oxidative stress mimics a physiological state in which the cells respond to this stress. Which receptors are involved in the sensing of this redox status? Are these sensors the same as those involved in the sensing of reactive oxygen species? These two questions need to be addressed.

In summary, we have shown that Gex1 is a proton antiporter directly participating in cell survival under oxidative stress conditions through the mediation of detoxification and/or glutathione homeostasis. We have also shown that Gex1 production is regulated by the iron-responsive factor Aft2 and that pH and thiol-redox changes induced by Gex1 modulate the PKA and PKC1-MAPK pathways. We believe that the cytosolic changes induced by Gex1 also influence its intracellular distribution, although this remains to be demonstrated definitively.

MATERIALS AND METHODS

Yeast strains and plasmid construction

The *S. cerevisiae* strains used in this study are listed in Table 1. All are derivatives of BY4741/BY4742.

Deletion strains and strains carrying GFP- or 6HA-tagged genes were constructed by one-step gene replacement with PCR-generated cassettes (Longtine *et al.*, 1998; Janke *et al.*, 2004). The *gex1Δ gex2Δ* strain was obtained by the disruption of *GEX1* and *GEX2* in haploid strains (BY4741 and BY4742), which were then crossed and allowed to sporulate for tetrad analysis.

The p*GEX1-GFP* and p*GEX1-HA* plasmids were obtained by inserting a fragment encoding *GEX1* in frame with the *GFP* or *6HA* coding sequence into the centromeric p416-GAL vector (pØ) (Mumberg *et al.*, 1994). These fragments were obtained by PCR, with genomic DNA from the chromosomally tagged strains used as the template.

The centromeric pCM188 plasmid was used to clone the wild-type *AFT1*, *AFT2* and the mutant *AFT1–1^{up}*, *AFT2–1^{up}* alleles under the control of the doxycycline-regulated promoter (Garí *et al.*, 1997). The p*AFT1* and p*AFT1–1^{up}* plasmids were constructed by inserting PCR-amplified fragments containing either the wild-type *AFT1* or the Cys291Phe-mutated *AFT1–1^{up}* coding sequence into pCM188. These fragments were obtained by PCR amplification of genomic DNA from the CM3260 and M2 strains (Yamaguchi-Iwai *et al.*, 1995).

The pEG202-*AFT2* plasmid (Blaiseau *et al.*, 2001) was used as a template to generate the *AFT2–1^{up}* allele (Cys187Phe mutated) with the QuikChange Site-Directed Mutagenesis Kit (Stratagene, La Jolla, CA). Plasmids p*AFT2* and p*AFT2–1^{up}* were constructed by inserting the *AFT2* and *AFT2–1^{up}* coding sequences into pCM188. The other plasmids used in this study were YEp351-*YAP1* (p*YAP1*), pAW18 (p*YAP2*) (Lesuisse and Labbe, 1995), pADH1-*MSN2-GFP* (Görner *et al.*, 1998), and p*ADH1-pHluorin* (Dechant *et al.*, 2010).

Growth conditions

Yeast cells were grown at 30°C in rich medium (YP): 1% yeast extract, 2% peptone, supplemented with 2% glucose (YPD) or 2% galactose (YPG). Cells transformed with plasmids were grown in minimal medium (YNB) containing 0.67% yeast nitrogen base without amino acids (Difco; BD, Franklin Lakes, NJ) and supplemented with the appropriate nutrients. The carbon source was 2% glucose, raffinose, or galactose. Unless stated, cells bearing pØ, p*GEX1-HA*, or p*GEX1-GFP* plasmids were grown in the presence of galactose as a carbon source to induce the galactose promoter. For BPS (Sigma-Aldrich, St. Louis, MO) treatments, cells were incubated with 200 µM BPS overnight.

Yeast cell extracts, SDS–PAGE, Western immunoblotting, and antibodies

Total protein extracts were prepared by the NaOH/trichloroacetic acid lysis technique (Volland *et al.*, 1994). Proteins were separated by SDS–PAGE in 10% tricine gels or commercial precast gels (NuPAGE 4–12% Bis–Tris gels with morpholino propane sulfonic acid buffer; Invitrogen, Carlsbad, CA) and transferred onto nitrocellulose membranes. The antibodies used were monoclonal anti-GFP (clones 7.1 and 13.1; Roche Diagnostics, Indianapolis, IN) and anti-HA (clone F-7; Santa Cruz Biotechnology, Santa Cruz, CA), polyclonal anti-Vph1 (10D7, Invitrogen), anti-PGK (NE130/7S, Nordic Immunology, Tilburg, Netherlands), anti–phospho-p44/42 MAPK (4370; Cell Signaling Technology, Beverly, MA), and anti-Pma1 (a gift from Caroline Slayman) antibodies. Primary antibodies were detected with secondary antibodies conjugated to horseradish peroxidase (Sigma-Aldrich). Immunoblotting images were acquired with the LAS-4000 imaging system (Fujifilm, Tokyo, Japan), and band intensities were quantified with ImageJ software.

Sucrose density gradients

Sucrose density gradients were prepared as previously described (Erpapazoglou *et al.*, 2008).

Fluorescence microscopy

Fluorescence observations were performed with an Olympus BY61 microscope (Olympus, Tokyo, Japan) equipped with a fluorescein isothiocyanate (FITC) filter set (Filter 41001 FITC, Exciter HQ480/40x, Dichroic Q505LP, and Emitter HQ535/50 nm; Chroma Technology, Bellows Falls, VT) for GFP, NBD-Ga-DFOB, pHluorin, and quinacrine and a 4′,6-diamidino-2-phenylindole (DAPI) filter set (Filter 31013v2 DAPI, Exciter D365/40x, Dichroic 400DCLP, and Emitter D460/50 nm; Chroma Technology) for 7-amino-4-chloromethylcoumarin (CMAC). Cell shape was visualized with Nomarski optics. Images were acquired with a SPOT4.05 charge-coupled device camera. Images were processed with ImageJ, Adobe Photoshop CS3, and Adobe Illustrator CS3.

For cytosolic pH measurement, cells were transformed with *pADH1-pHluorin* encoding the ratiometric pHluorin (Miesenböck *et al.*, 1998; Dechant *et al.*, 2010). Cells were grown to midexponential growth phase in YNB, and fluorescence was measured with a Photon Technology International (Birmingham, NJ) monochromator and Felix 32 software. Fluorescence emission was read at 508 nm, and the ratio of the emission obtained at two excitation wavelengths (410 nm [I_{410}] and 470 nm [I_{470}]) was calculated. The same cells were observed by fluorescence microscopy with the FITC filter set.

The vacuole lumen was visualized by incubating the cells with 5 µM Cell Tracker Blue CMAC (Molecular Probes, Eugene, OR) for 15 min at 30°C and washing the cells with minimal medium. Acidification of the vacuole was assayed with the pH-sensitive fluorescent probe quinacrine [*N*′-(6-chloro-2-methoxy-acridin-9-yl)-*N*,*N*-diethylpentane-1,4-diamine] (Sigma-Aldrich), as previously described (Baggett *et al.*, 2003). For iodine staining, cells were grown on plates for 3 d and then gently covered with a solution of 0.2% iodine/0.4% potassium iodide. Photographs were taken 3 min later. The presence of glycogen resulted in a darkening of the yeast cells.

Quantification of iron, copper, and cadmium content

Iron, copper, and cadmium contents were quantified for all strains by the inductively coupled plasma mass spectrometry method as carried out at the Service Central d'Analyse du CNRS (Solaize, France).

Determination of glutathione levels (GSH plus GSSG)

Glutathione levels were determined as previously described (Auchère *et al.*, 2008).

Yeast strains were grown in minimum medium as previously described (Perrone *et al.*, 2005), and cells were harvested at the appropriate growth phase by centrifugation. Extracellular glutathione concentration was measured directly in the resulting supernatant. For the estimation of total intracellular glutathione content, cell pellets were washed and resuspended in ice-cold 5% 5-sulfosalicylic acid in 50 mM potassium phosphate buffer, pH 7.8, and disrupted with glass beads. For the estimation of total intracellular glutathione concentration, cell pellets were washed and resuspended in 50 mM potassium phosphate buffer, pH 7.8, containing 5% ice-cold 5-sulfosalicylic acid and disrupted with glass beads. The resulting mixture was clarified by centrifugation (30 min, 5000 × *g*, 4°C), and the supernatant was used to determine total free glutathione (reduced and oxidized) concentration. A typical reaction mixture contained the cell extract, 20 mM DTNB, and 10 mM NADPH in 50 mM potassium phosphate buffer, pH 7.8. The reaction was started by adding glutathione reductase (1.5 U/ml), and the kinetics of DTNB conversion to TNB was followed spectrophotometrically at 412 nm. Glutathione concentrations were calculated from standard curves obtained with various GSSG concentrations based on rates of TNB formation and are expressed as nmol of glutathione/mg of protein. GSH:GSSG ratios were calculated using the equation GSH/GSSG = 2(total glutathione)/GSSG.

All data points in the figures and the values listed are means of at least six determinations, and Student's *t* test was used to identify significant differences.

ACKNOWLEDGMENTS

We thank Michel Jacquet (Institut de Génétique et Microbiologie, CNRS/UPS UMR 8621, Paris, France) and Myriam Ruault (Institut Curie, Paris) for helpful discussions. We also thank R. Dechant (Institute of Biochemistry, ETH Zurich, Zurich, Switzerland) for the p*ADH1-pHluorin* construct and M. Jacquet for p*ADH1-MSN2-GFP*. We thank Zoi Erpapazoglou (Institut Jacques-Monod, Paris) for stimulating discussions. We thank members of the laboratory for critical reading of the manuscript and Alex Edelman & Associates for editorial assistance. This work was supported by the Centre

National de la Recherche Scientifique and the Université Paris-Diderot. Experiments performed in laboratory of R.H.-T. were supported by grant 3298 from the Association pour la Recherche sur le Cancer and by a grant from the European Network VI Framework (Role of Ubiquitin and Ubiquitin-like Modifiers in Cellular Regulation, contract no. 018683). Manel Dhaoui received a fellowship from the Tunisian Ministry of Research and the Region Ile-de-France.

REFERENCES

Auchère F, Santos R, Planamente S, Lesuisse E, Camadro J-M (2008). Glutathione-dependent redox status of frataxin-deficient cells in a yeast model of Friedreich's ataxia. Hum Mol Genet 17, 2790–2802.

Baggett JJ, Shaw JD, Sciambi CJ, Watson HA, Wendland B (2003). Fluorescent labeling of yeast. Curr Protoc Cell Biol Chapter 4, Unit 4.13.

Ballatori N, Hammond CL, Cunningham JB, Krance SM, Marchan R (2005). Molecular mechanisms of reduced glutathione transport: role of the MRP/CFTR/ABCC and OATP/SLC21A families of membrane proteins. Toxicol Appl Pharmacol 204, 238–255.

Belcastro M, Marino T, Russo N, Toscano M (2009). The role of glutathione in cadmium ion detoxification: coordination modes and binding properties—a density functional study. J Inorg Biochem 103, 50–57.

Blaiseau PL, Lesuisse E, Camadro JM (2001). Aft2p, a novel iron-regulated transcription activator that modulates, with Aft1p, intracellular iron use and resistance to oxidative stress in yeast. J Biol Chem 276, 34221–34226.

Blaiseau PL, Seguin A, Camadro J, Lesuisse E (2010). Iron uptake in yeasts. In: Iron Uptake and Homeostasis in Microorganisms, ed. Cornelis P, Andrews SC, Norfolk, United Kingdom: Caister Academic Press, 1–20.

Blondel M-O, Morvan J, Dupré S, Urban-Grimal D, Haguenauer-Tsapis R, Volland C (2004). Direct sorting of the yeast uracil permease to the endosomal system is controlled by uracil binding and Rsp5p-dependent ubiquitylation. Mol Biol Cell 15, 883–895.

Boll M, Daniel H, Gasnier B (2004). The SLC36 family: proton-coupled transporters for the absorption of selected amino acids from extracellular and intracellular proteolysis. Pflugers Arch 447, 776–779.

Bonifacino JS, Traub LM (2003). Signals for sorting of transmembrane proteins to endosomes and lysosomes. Annu Rev Biochem 72, 395–447.

Brett CL, Tukaye DN, Mukherjee S, Rao R (2005). The yeast endosomal Na^+K^+/H^+ exchanger Nhx1 regulates cellular pH to control vesicle trafficking. Mol Biol Cell 16, 1396–1405.

Chen Y, Feldman DE, Deng C, Brown JA, De Giacomo AF, Gaw AF, Shi G, Le QT, Brown JM, Koong AC (2005). Identification of mitogen-activated protein kinase signaling pathways that confer resistance to endoplasmic reticulum stress in *Saccharomyces cerevisiae*. Mol Cancer Res 3, 669–677.

Cohen BA, Pilpel Y, Mitra RD, Church GM (2002). Discrimination between paralogs using microarray analysis: application to the Yap1p and Yap2p transcriptional networks. Mol Biol Cell 13, 1608–1614.

Courel M, Lallet S, Camadro J-M, Blaiseau P-L (2005). Direct activation of genes involved in intracellular iron use by the yeast iron-responsive transcription factor Aft2 without its paralog Aft1. Mol Cell Biol 25, 6760–6771.

Dechant R, Binda M, Lee SS, Pelet S, Winderickx J, Peter M (2010). Cytosolic pH is a second messenger for glucose and regulates the PKA pathway through V-ATPase. EMBO J 29, 2515–2526.

Dupré S, Urban-Grimal D, Haguenauer-Tsapis R (2004). Ubiquitin and endocytic internalization in yeast and animal cells. Biochim Biophys Acta 1695, 89–111.

Erpapazoglou Z, Froissard M, Nondier I, Lesuisse E, Haguenauer-Tsapis R, Belgareh-Touzé N (2008). Substrate- and ubiquitin-dependent trafficking of the yeast siderophore transporter Sit1. Traffic 9, 1372–1391.

Fabre E, Muller H, Therizols P, Lafontaine I, Dujon B, Fairhead C (2005). Comparative genomics in hemiascomycete yeasts: evolution of sex, silencing, and subtelomeres. Mol Biol Evol 22, 856–873.

Froissard M, Belgareh-Touzé N, Dias M, Buisson N, Camadro J-M, Haguenauer-Tsapis R, Lesuisse E (2007). Trafficking of siderophore transporters in *Saccharomyces cerevisiae* and intracellular fate of ferrioxamine B conjugates. Traffic 8, 1601–1616.

Garí E, Piedrafita L, Aldea M, Herrero E (1997). A set of vectors with a tetracycline-regulatable promoter system for modulated gene expression in *Saccharomyces cerevisiae*. Yeast 13, 837–848.

Gaxiola RA, Yuan DS, Klausner RD, Fink GR (1998). The yeast CLC chloride channel functions in cation homeostasis. Proc Natl Acad Sci USA 95, 4046–4050.

Ghosh M, Shen J, Rosen BP (1999). Pathways of As(III) detoxification in *Saccharomyces cerevisiae*. Proc Natl Acad Sci USA 96, 5001–5006.

Goffeau A, Park J, Paulsen IT, Jonniaux JL, Dinh T, Mordant P, Saier MH (1997). Multidrug-resistant transport proteins in yeast: complete inventory and phylogenetic characterization of yeast open reading frames with the major facilitator superfamily. Yeast 13, 43–54.

Görner W, Durchschlag E, Martinez-Pastor MT, Estruch F, Ammerer G, Hamilton B, Ruis H, Schüller C (1998). Nuclear localization of the C2H2 zinc finger protein Msn2p is regulated by stress and protein kinase A activity. Genes Dev 12, 586–597.

Gottschling DE, Aparicio OM, Billington BL, Zakian VA (1990). Position effect at *S. cerevisiae* telomeres: reversible repression of Pol II transcription. Cell 63, 751–762.

Grant CM, MacIver FH, Dawes IW (1996). Glutathione is an essential metabolite required for resistance to oxidative stress in the yeast *Saccharomyces cerevisiae*. Curr Genet 29, 511–515.

Greene JR, Brown NH, DiDomenico BJ, Kaplan J, Eide DJ (1993). The *GEF1* gene of *Saccharomyces cerevisiae* encodes an integral membrane protein; mutations in which have effects on respiration and iron-limited growth. Mol Gen Genet 241, 542–553.

Gromadka R, Gora M, Zielenkiewicz U, Slonimski PP, Rytka J (1996). Subtelomeric duplications in *Saccharomyces cerevisiae* chromosomes III and XI: topology, arrangements, corrections of sequence and strain-specific polymorphism. Yeast 12, 583–591.

Gueldry O, Lazard M, Delort F, Dauplais M, Grigoras I, Blanquet S, Plateau P (2003). Ycf1p-dependent Hg(II) detoxification in *Saccharomyces cerevisiae*. Eur J Biochem 270, 2486–2496.

Haas H, Eisendle M, Turgeon BG (2008). Siderophores in fungal physiology and virulence. Annu Rev Phytopathol 46, 149–187.

Halliwell B, Gutteridge JM (1984). Oxygen toxicity, oxygen radicals, transition metals and disease. Biochem J 219, 1–14.

Herrero E, Ros J, Bellí G, Cabiscol E (2008). Redox control and oxidative stress in yeast cells. Biochim Biophys Acta 1780, 1217–1235.

Heymann P, Ernst JF, Winkelmann G (1999). Identification of a fungal triacetylfusarinine C siderophore transport gene (*TAF1*) in *Saccharomyces cerevisiae* as a member of the major facilitator superfamily. Biometals 12, 301–306.

Heymann P, Ernst JF, Winkelmann G (2000a). A gene of the major facilitator superfamily encodes a transporter for enterobactin (Enb1p) in *Saccharomyces cerevisiae*. Biometals 13, 65–72.

Heymann P, Ernst JF, Winkelmann G (2000b). Identification and substrate specificity of a ferrichrome-type siderophore transporter (Arn1p) in *Saccharomyces cerevisiae*. FEMS Microbiol Lett 186, 221–227.

Homolya L, Varadi A, Sarkadi B (2003). Multidrug resistance-associated proteins: export pumps for conjugates with glutathione, glucuronate or sulfate. Biofactors 17, 103–114.

Janke C *et al.* (2004). A versatile toolbox for PCR-based tagging of yeast genes: new fluorescent proteins, more markers and promoter substitution cassettes. Yeast 21, 947–962.

Jungwirth H, Kuchler K (2006). Yeast ABC transporters—a tale of sex, stress, drugs and aging. FEBS Lett 580, 1131–1138.

Lauwers E, Erpapazoglou Z, Haguenauer-Tsapis R, André B (2010). The ubiquitin code of yeast permease trafficking. Trends Cell Biol 20, 196–204.

Lesage G, Shapiro J, Specht CA, Sdicu A-M, Ménard P, Hussein S, Tong AHY, Boone C, Bussey H (2005). An interactional network of genes involved in chitin synthesis in *Saccharomyces cerevisiae*. BMC Genet 6, 81–16.

Lesuisse E, Blaiseau PL, Dancis A, Camadro JM (2001). Siderophore uptake and use by the yeast *Saccharomyces cerevisiae*. Microbiology 147, 289–298.

Lesuisse E, Labbe P (1995). Effects of cadmium and of *YAP1* and *CAD1/YAP2* genes on iron metabolism in the yeast *Saccharomyces cerevisiae*. Microbiology 141, 2937–2943.

Lesuisse E, Simon-Casteras M, Labbe P (1998). Siderophore-mediated iron uptake in *Saccharomyces cerevisiae*: the *SIT1* gene encodes a ferrioxamine B permease that belongs to the major facilitator superfamily. Microbiology 144, 3455–3462.

Li ZS, Szczypka M, Lu YP, Thiele DJ, Rea PA (1996). The yeast cadmium factor protein (YCF1) is a vacuolar glutathione S–conjugate pump. J Biol Chem 271, 6509–6517.

Liu XF, Culotta VC (1999). Mutational analysis of *Saccharomyces cerevisiae* Smf1p, a member of the Nramp family of metal transporters. J Mol Biol 289, 885–891.
Longtine MS, McKenzie A, Demarini DJ, Shah NG, Wach A, Brachat A, Philippsen P, Pringle JR (1998). Additional modules for versatile and economical PCR-based gene deletion and modification in *Saccharomyces cerevisiae*. Yeast 14, 953–961.
Lopez-Rodriguez A, Trejo AC, Coyne L, Halliwell RF, Miledi R, Martinez-Torres A (2007). The product of the gene *GEF1* of *Saccharomyces cerevisiae* transports Cl– across the plasma membrane. FEMS Yeast Res 7, 1218–1229.
Martín H, Flández M, Nombela C, Molina M (2005). Protein phosphatases in MAPK signalling: we keep learning from yeast. Mol Microbiol 58, 6–16.
Miesenböck G, De Angelis DA, Rothman JE (1998). Visualizing secretion and synaptic transmission with pH-sensitive green fluorescent proteins. Nature 394, 192–195.
Mumberg D, Muller R, Funk M (1994). Regulatable promoters of *Saccharomyces cerevisiae*: comparison of transcriptional activity and their use for heterologous expression. Nucleic Acids Res 22, 5767–5768.
Nagy Z, Montigny C, Leverrier P, Yeh S, Goffeau A, Garrigos M, Falson P (2006). Role of the yeast ABC transporter Yor1p in cadmium detoxification. Biochimie 88, 1665–1671.
Panwar SL, Pasrija R, Prasad R (2008). Membrane homoeostasis and multidrug resistance in yeast. Biosci Rep 28, 217–228.
Pao SS, Paulsen IT, Saier MH (1998). Major facilitator superfamily. Microbiol Mol Biol Rev 62, 1–34.
Paumi CM, Chuk M, Snider J, Stagljar I, Michaelis S (2009). ABC transporters in *Saccharomyces cerevisiae* and their interactors: new technology advances the biology of the ABCC (MRP) subfamily. Microbiol Mol Biol Rev 73, 577–593.
Penninckx MJ (2002). An overview on glutathione in *Saccharomyces* versus non-conventional yeasts. FEMS Yeast Res 2, 295–305.
Perrone GG, Grant CM, Dawes IW (2005). Genetic and environmental factors influencing glutathione homeostasis in *Saccharomyces cerevisiae*. Mol Biol Cell 16, 218–230.
Philpott CC (2006). Iron uptake in fungi: a system for every source. Biochim Biophys Acta 1763, 636–645.
Philpott CC, Protchenko O, Kim YW, Boretsky Y, Shakoury-Elizeh M (2002). The response to iron deprivation in *Saccharomyces cerevisiae*: expression of siderophore-based systems of iron uptake. Biochem Soc Trans 30, 698–702.
Pocsi I, Prade RA, Penninckx MJ (2004). Glutathione, altruistic metabolite in fungi. Adv Microb Physiol 49, 1–76.
Polec-Pawlak K, Ruzik R, Lipiec E (2007). Investigation of Cd(II), Pb(II) and Cu(I) complexation by glutathione and its component amino acids by ESI-MS and size exclusion chromatography coupled to ICP-MS and ESI-MS. Talanta 72, 1564–1572.
Rutherford JC, Jaron S, Ray E, Brown PO, Winge DR (2001). A second iron-regulatory system in yeast independent of Aft1p. Proc Natl Acad Sci USA 98, 14322–14327.
Sagne C, Agulhon C, Ravassard P, Darmon M, Hamon M, El Mestikawy S, Gasnier B, Giros B (2001). Identification and characterization of a lysosomal transporter for small neutral amino acids. Proc Natl Acad Sci USA 98, 7206–7211.
Salin H, Fardeau V, Piccini E, Lelandais G, Tanty V, Lemoine S, Jacq C, Devaux F (2008). Structure and properties of transcriptional networks driving selenite stress response in yeasts. BMC Genomics 9, 333.
Scandalios JG (2002). Oxidative stress responses—what have genome-scale studies taught us? Genome Biol 3, 1019.1–1019.5.
Schwappach B, Stobrawa S, Hechenberger M, Steinmeyer K, Jentsch TJ (1998). Golgi localization and functionally important domains in the NH2 and COOH terminus of the yeast CLC putative chloride channel Gef1p. J Biol Chem 273, 15110–15118.
Sipos K, Lange H, Fekete Z, Ullmann P, Lill R, Kispal G (2002). Maturation of cytosolic iron–sulfur proteins requires glutathione. J Biol Chem 277, 26944–26949.
Smith A, Ward MP, Garrett S (1998). Yeast PKA represses Msn2p/Msn4p-dependent gene expression to regulate growth, stress response and glycogen accumulation. EMBO J 17, 3556–3564.
Sychrova H, Ramirez J, Pena A (1999). Involvement of Nha1 antiporter in regulation of intracellular pH in *Saccharomyces cerevisiae*. FEMS Microbiol Lett 171, 167–172.
Szczypka MS, Wemmie JA, Moye-Rowley WS, Thiele DJ (1994). A yeast metal resistance protein similar to human cystic fibrosis transmembrane conductance regulator (CFTR) and multidrug resistance-associated protein. J Biol Chem 269, 22853–22857.
Temple MD, Perrone GG, Dawes IW (2005). Complex cellular responses to reactive oxygen species. Trends Cell Biol 15, 319–326.
Vilella F, Herrero E, Torres J, de la Torre-Ruiz MA (2005). Pkc1 and the upstream elements of the cell integrity pathway in *Saccharomyces cerevisiae*, Rom2 and Mtl1, are required for cellular responses to oxidative stress. J Biol Chem 280, 9149–9159.
Volland C, Urban-Grimal D, Géraud G, Haguenauer-Tsapis R (1994). Endocytosis and degradation of the yeast uracil permease under adverse conditions. J Biol Chem 269, 9833–9841.
Walter PB, Knutson MD, Paler-Martinez A, Lee S, Xu Y, Viteri FE, Ames BN (2002). Iron deficiency and iron excess damage mitochondria and mitochondrial DNA in rats. Proc Natl Acad Sci USA 99, 2264–2269.
Wemmie JA, Szczypka MS, Thiele DJ, Moye-Rowley WS (1994). Cadmium tolerance mediated by the yeast AP-1 protein requires the presence of an ATP-binding cassette transporter-encoding gene, YCF1. J Biol Chem 269, 32592–32597.
Winkelmann G (2001). Siderophore transport in fungi. In: Microbial Transport Systems, ed. Winkelmann G, Weinheim, Germany: Wiley-VCH, 463–481.
Wu AL, Moye-Rowley WS (1994). GSH1, which encodes gamma-glutamylcysteine synthetase, is a target gene for yAP-1 transcriptional regulation. Mol Cell Biol 14, 5832–5839.
Wyrick JJ, Holstege FC, Jennings EG, Causton HC, Shore D, Grunstein M, Lander ES, Young RA (1999). Chromosomal landscape of nucleosome-dependent gene expression and silencing in yeast. Nature 402, 418–421.
Wysocki R, Tamás MJ (2010). How *Saccharomyces cerevisiae* copes with toxic metals and metalloids. FEMS Microbiol Rev 34, 925–951.
Yamaguchi-Iwai Y, Dancis A, Klausner RD (1995). *AFT1*: a mediator of iron regulated transcriptional control in *Saccharomyces cerevisiae*. EMBO J 14, 1231–1239.
Yun CW, Ferea T, Rashford J, Ardon O, Brown PO, Botstein D, Kaplan J, Philpott CC (2000a). Desferrioxamine-mediated iron uptake in *Saccharomyces cerevisiae*. Evidence for two pathways of iron uptake. J Biol Chem 275, 10709–10715.
Yun CW, Tiedeman JS, Moore RE, Philpott CC (2000b). Siderophore-iron uptake in *Saccharomyces cerevisiae*. Identification of ferrichrome and fusarinine transporters. J Biol Chem 275, 16354–16359.